

Impact of Lewis Acids on Diels–Alder Reaction Reactivity: A Conceptual Density Functional Theory Study

Yue Xia,[†] Dulin Yin,^{*,†} Chunying Rong,[†] Qiong Xu,[†] Donghong Yin,[†] and Shubin Liu^{*,†,‡}

Key Laboratory of Chemical Biology and Traditional Chinese Medicine Research, Ministry of Education, College of Chemistry and Chemical Engineering, Hunan Normal University, Changsha, Hunan 410081, P. R. China, Renaissance Computing Institute, University of North Carolina, Chapel Hill, North Carolina 27599-3455, and Division of Research Computing, Information Technology Services, University of North Carolina, 211 Manning Drive, Chapel Hill, North Carolina 27599-3420

Received: June 17, 2008; Revised Manuscript Received: August 4, 2008

Density functional theory (DFT) and conceptual/chemical DFT studies are carried out in this work for the normal electron demand Diels–Alder reaction between isoprene and acrolein to compare chemical reactivity and regioselectivity of the reactants in the absence and presence of Lewis acid (LA) catalysts. A cyclic coplanar structure of acrolein–LA complex has been observed and the natural bond orbital analysis has been employed to interpret the interaction between acrolein and LAs. Reactivity indices from frontier molecular orbital energies are proved to be adequate and efficient to evaluate the catalytic property of LAs. Linear relationships have been discovered among the bond order, bond length, catalytic activation, and chemical reactivity for the systems concerned. The validity and applicability of maximum hardness principle, minimum polarizability principle, and minimum electrophilicity principle are examined and discussed in the prediction of the major regioselective isomer and the preferred reaction pathway for the reactions in the present study.

1. Introduction

Diels–Alder (DA) reaction,^{1–5} involving a large variety of dienes and dienophiles, is one of the most powerful methods in the organic synthesis of six-membered functionalized carbocyclic compounds, especially in the preparation of structurally complex and physiologically active natural products with high stereospecificity and stereoselectivity.^{4,5} The interaction between unsymmetrical dienes and dienophiles in DA reactions can yield two regioselective products depending on the orientation of the substituents in the adduct. For instance, 1- and 2-substituted butadienes reacting with monosubstituted dienophiles can yield *ortho* and *para* adducts, respectively. Frontier molecular orbital (FMO) theory^{2,6–8} and reactivity modeling⁹ based on the matching of complementary reactivity surfaces for diene and dienophile provide reasonable rationalization about the cycloadduct regiochemistry. Secondary orbital interactions¹⁰ were also proposed to contribute to the regioselectivity of the DA reaction between unsymmetrically substituted dienes and dienophiles.

The Lewis acid (LA) catalysis of DA reactions is of considerable interest in the literature.^{11–15} Since the remarkable acceleration of DA reaction catalyzed by AlCl₃ was first reported by Yates and Eaton,¹¹ LA catalysis in DA reactions has attained much attention due to its striking rate acceleration and high regio- and stereoselectivities in comparison with the uncatalyzed process.^{1,2,12,13} FMO theory^{2,14} and secondary orbital interactions¹⁵ were utilized to rationalize the catalytic effect of LAs on reaction rate acceleration, regioselectivity, and stereoselectivity via orbital coefficients remixing.

Theoretical calculations using semiempirical,¹⁶ *ab initio*^{17–19} and density functional theory (DFT)^{20–22} approaches are capable of obtaining valuable insights into the role of LAs in the mechanistic aspects and shedding light on understanding the reactivity and selectivity for DA reactions. It has been predicted that the LA catalyst enables a notable increase in the asynchronicity of the transition state and a significant decrease in the activation energy, as compared with the uncatalyzed counterpart. Conceptual DFT^{23,24} has been used to examine and understand the chemical reactivity and site selectivity of the molecular systems. In this context, global reactivity indicators such as electronegativity, global hardness, and electrophilicity index together with local quantities such as local softness, Fukui functions, and local electrophilicity index, etc., have been utilized to address chemical reactivity and site selectivity.^{25–30} Domingo et al.²⁸ have shown that the classification of diene/dienophile pairs with a unique scale of electrophilicity is a useful tool for predicting the reaction mechanism and regioselectivity of DA reactions. They have also extended the global electrophilicity index to deal with the local or regional counterpart of this property.²⁹ Similarly, HSAB (hard and soft acid and base) principle³⁰ has been employed to interpret the orientation difference in cycloaddition reactions. Recently, maximum hardness principle (MHP), minimum polarizability principle (MPP),^{31–35} and very recently, minimum electrophilicity principle (MEP)^{36–40} have been introduced to explore the chemical reactivity and direction to which a chemical reaction evolves. Noorizadeh and Mairami³⁷ have used DFT based reactivity descriptors such as hardness, polarizability and electrophilicity to predict the stability sequence of the regioselective products in a series of DA reactions and found that the major product always possesses a smaller electrophilicity than the minor product. On the basis of the findings, they claimed that the electrophilicity index can be used as an indicator of regioselectivity for this type of reactions. Also, Noorizadeh³⁸ has

* Corresponding authors. E-mail: dulinyin@126.com (D.L.Y.) and shubin@email.unc.edu (S.B.L.).

[†] Hunan Normal University.

[‡] Renaissance Computing Institute and Information Technology Services, University of North Carolina.

investigated 25 simple reactions and found that for those chemical reactions in which the number of moles decreases or at least remains constant, the most stable species (reactants or products) have the lowest sum of electrophilicities, in accordance with MEP. MEP has also been successfully applied to predict the regioselectivity for photocycloaddition and stereoisomerization reactions.³⁹

In this paper, the commonly used traditional LAs such as chlorides of aluminum, boron, zinc, copper, etc. are adopted in the DA reaction between isoprene and acrolein. Global reactivity descriptors such as chemical potential μ , global hardness η , polarizability α , electrophilicity index ω , as well as local reactivity descriptors like Fukui functions f_k^α and local electrophilicity indices ω_k have been calculated to investigate the impacts of different LA catalysts on the reactivity and regioselectivity of the studied DA reactions. Structure and natural bond orbital (NBO) analyses are carried out to understand the nature of the interactions between acrolein and LA catalysts. A few linear relationships between structure and reactivity properties for the LA catalysts are established. MHP, MPP and MEP have also been applied to evaluate the validity and applicability of the three principles for these reactions in the prediction of the major regioproduct and the preferred reaction pathway.

2. Theoretical Background

DFT reactivity indices can play a central role in the understanding of chemical reactivity and regioselectivity of a molecule. In the context of conceptual DFT,^{23,24} the commonly used indices are the chemical potential μ , global hardness η , and polarizability α , whose analytical definitions are defined as follows:

$$\mu = -\chi = \left(\frac{\partial E}{\partial N} \right)_v = -\frac{1}{2}(I + A) \quad (1)$$

$$\eta = \left(\frac{\partial^2 E}{\partial N^2} \right)_v = \left(\frac{\partial \mu}{\partial N} \right)_v = I - A \quad (2)$$

$$\langle \alpha \rangle = \frac{1}{3}(\alpha_{xx} + \alpha_{yy} + \alpha_{zz}) \quad (3)$$

where E is the total energy of the system, N is the number of electrons in the system, v is the external potential, I and A are the first ionization potential and electron affinity, respectively, and $\langle \alpha \rangle$ is the mean of diagonal components (α_{xx} , α_{yy} and α_{zz}) of the polarizability tensor.^{37,38} Here, the first ionization potential I can be obtained by $I = E_{N-1} - E_N$ and electron affinity A by $A = E_{N+1} - E_N$ with E_{N+1} , E_{N-1} , and E_N denoting the total energies of the system with $N + 1$, $N - 1$, and N electrons, respectively. In addition, following Janak's theorem,⁴¹ the first ionization potential I and electron affinity A can be replaced by the frontier molecular orbital energies HOMO (ε_H) and LUMO (ε_L), respectively. Chemical potential, μ , and global hardness, η , can thus be expressed as follows:

$$\mu \approx \frac{\varepsilon_L + \varepsilon_H}{2} \quad (4)$$

$$\eta \approx \varepsilon_L - \varepsilon_H \quad (5)$$

Parr et al.²⁵ have introduced electrophilicity index ω , in terms of μ and η to appraise the capacity of an electrophile to accept the maximal number electrons in a neighboring reservoir of electron sea,

$$\omega = \frac{\mu^2}{2\eta} \quad (6)$$

To describe the regioselectivity, local descriptors have to be employed. A well-known local descriptor of this category is called Fukui function,⁴² which is defined as

$$f(r) = \left(\frac{\partial \rho(r)}{\partial N} \right)_{v(r)} = \left(\frac{\partial \mu}{\partial v(r)} \right)_N \quad (7)$$

The condensed forms of Fukui functions proposed by Yang and Mortier⁴³ are based on a population analysis under the finite difference approximation, e.g., NBO analysis. For systems with electron gain, the condensed Fukui index is of nucleophilic nature:

$$f_k^+ = q_k(N + 1) - q_k(N) \quad (8)$$

For systems with electron donation, the condensed Fukui index is a measure of the electrophilic attack:

$$f_k^- = q_k(N) - q_k(N - 1) \quad (9)$$

where $q_k(N + 1)$, $q_k(N)$, and $q_k(N - 1)$ stand for the gross NBO population on Atom k in a molecule with $N + 1$, N , and $N - 1$ electrons, respectively. A local electrophilicity index ω_k expressed as

$$\omega_k = \omega f_k^+ \quad (10)$$

is considered to be better suited to analyze reactivity and selectivity for reactions involving electrophile–nucleophile interactions.²⁶

To examine the validity and applicability of MHP, MPP, and MEP for chemical reactions of the present study, the difference, ΔY , of a DFT reactivity descriptor Y ($Y = \eta$, $\langle \alpha \rangle$, or ω) between reactants and products is defined as³⁷

$$\Delta Y = \sum_i v_i Y_i \quad (11)$$

where v_i stands for the stoichiometry coefficient of the i th participant of the reaction and Y_i is the value of parameter Y for the i th compound in the considered reaction. The sign of v_i will be positive if the i th species is a product; otherwise it is negative. A maximum principle of the descriptor Y for a chemical reaction, if existent, requires that ΔY is larger than zero, $\Delta Y > 0$, and conversely a minimum principle implies that $\Delta Y < 0$.

To assess catalytic capability of an LA and its accelerating effect on the DA reaction, following the literature^{14,18,20,44} and using frontier molecular orbitals, we hereby define two quantities, ΔE_a and ΔE . The DA reaction between isoprene and acrolein is controlled by the gap between diene's HOMO, HOMO_{diene} and dienophile's LUMO, LUMO_{dienophile}. The presence of an LA induces a significant cutback in the activation energy, which can be understood in terms of stronger interactions between HOMO_{diene} and LUMO_{dienophile}, leading to the decrement of the HOMO_{diene} – LUMO_{dienophile} gap.^{18,20} The activation barrier ΔE_a of a DA reaction can be estimated by this gap:⁴⁴

$$\Delta E_a = \text{LUMO}_{\text{dienophile}} - \text{HOMO}_{\text{diene}} \quad (12)$$

On the other hand, an LA lowers both HOMO and LUMO energies of the dienophile through an activated dienophile-LA complex,^{2,14,44} We appraise the activation capability of LA through

$$\Delta E = \text{LUMO}_{\text{LA}} - \text{HOMO}_{\text{acrolein}} \quad (13)$$

where ΔE is the energy difference between the LUMO energy of the LA and the HOMO energy of the dienophile, acrolein. A lower LUMO energy of the LA produces a lower energy barrier, leading to a better activation.⁴⁴ We caution that ΔE is different from ΔE_{a} , but they might be related as they are telling the two sides of the same story on the accelerating effect of a Lewis acid catalyst.

3. Computational Details

DA reactions in the presence of homogeneous LA catalysts often take place in the condensed phase, and thus any realistic modeling of these reactions to simulate the impact of LAs on the chemical reactivity should in principle require that simulations be carried out in the condensed phase as well. In this work, however, we employ a rather simplified, gas-phase-like model, where LAs are represented by one single molecule interacting directly with the C=O bond of the dienophile, acrolein. Similar models of this kind have also been proposed elsewhere in the literature.^{18–20}

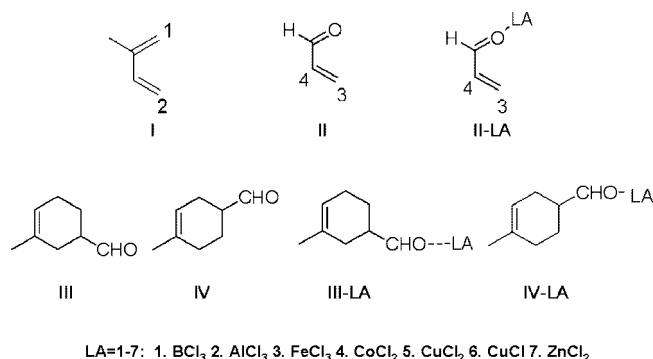
A series of LAs taken into account in the present study include two commonly used LAs, AlCl_3 and BCl_3 , and five transition metal chlorides, FeCl_3 , CoCl_2 , CuCl_2 , CuCl , and ZnCl_2 , whose structures are shown in Scheme 1. Isoprene was selected as a 2-substituted diene (I in Scheme 1), *s-cis*-acrolein^{17,20} and the corresponding *s-cis*-acrolein–LA complexes (II and II–LA in Scheme 1, respectively) were taken as dienophiles participating the uncatalyzed and LA-catalyzed reactions, respectively. The reaction between isoprene (I) and acrolein (II) is the so-called normal electron demand (NED) DA reaction,^{9,28,30} where I contains an electron-withdrawing carbonyl group (C=O) and II has an electron-donating methyl group (CH₃). Such a reaction yields two corresponding regioisomer products, *meta*-substituted product III and *para*-substituted product IV (Scheme 1). All equilibrium geometries of diene (I), dienophiles (II and II–LA), products (III and IV), and product–LA complexes (III–LA and IV–LA in Scheme 1) have been optimized at the DFT B3LYP level with Pople's 6-31 g* basis set. No imaginary frequency in the optimized conformations was found. Single-point frequency calculation and NBO analysis were carried out with the 6-311+g* basis set with tight SCF convergence using the optimized structure. Applicability of these basis sets to systems of this kind have been evaluated elsewhere.^{45–48}

For transition metal catalysts, such as FeCl_3 , CoCl_2 , CuCl_2 , and CuCl , different spin multiplicities^{45–50} are possible. Various spin states have been examined. Our results show that the high spin state for II– FeCl_3 ($S = 5/2$) and II– CoCl_2 ($S = 3/2$) is most stable, whereas for II– CuCl_2 and II– CuCl , the lowest spin state ($S = 1/2$ for CuCl_2 and $S = 0$ for CuCl) is the ground state. We employed the most stable spin state for each of the complexes in the present study. All calculations were performed using Gaussian 03 package.⁵¹

4. Results and Discussion

The reactivity difference between II and II–LA complexes (II–LAs) can be observed through comparison of their DFT reactivity indices and FMO energies shown in Table 1. Compared to II, we notice that (i) all II–LAs always have a larger electrophilicity index ω and smaller global hardness η , confirming that all II–LAs are more reactive than II; (ii) both HOMO and LUMO energies of II–LAs decrease except for the HOMO energy of II–6 (II– CuCl); the energy decrease in LUMO is more significant, justifying that it serves as the

SCHEME 1: Structure of Reactants and Products Involved in the Studied DA Reactions



primary electron acceptor in such $\text{HOMO}_{\text{diene}}-\text{LUMO}_{\text{dienophile}}$ -controlled DA reaction. The biggest LUMO energy decrease is 2.031 eV for acrolein– AlCl_3 (II–2). We use it as an example to compare the HOMO–LUMO interaction between I/II and I/II–LA, as illustrated in Figure 1, where one observes that, for the frontier orbital interaction between I and II, HOMO electrons (Figure 1A) are mainly localized on I and LUMO electrons (Figure 1B) on II. However, both HOMO and LUMO orbitals are diffused when AlCl_3 is present (Figure 1C,D), where electrons are transferred from double C=C bonds of I to the intermolecular regions and even to II due to the activation (electron attracting) effect of the LA.

According to the static model proposed by Domingo et al., the polarity of transition structure for a given DA reaction can be obtained from the difference in electrophilicity index ($\Delta\omega$) of the diene/dienophile interacting pair. A small $\Delta\omega$ value is an indication of a nonpolar mechanism, whereas a big $\Delta\omega$ value is associated with a polar mechanism.²⁸ From Table 1, we find that $\Delta\omega$ values between I and II–LAs are larger than those between I and II, suggesting that the DA reaction mechanism changes from an asynchronous concerted process to a stepwise mechanism when LA catalysts are existent.^{26,27} For such a polar characteristic of the interaction between the diene and dienophile pair, the new C–C bond formation prefers between the more nucleophilic site of diene and the more electrophilic site of dienophile. The C3 atom (see Table 1 and Scheme 1 for atom numbering) in all dienophiles (II and II–LA) is the preferential electrophilic site for nucleophilic attack as measured by both the large f_k^+ and ω_k values, whereas the nucleophilic site of isoprene is the C1 atom with largest value of f_k^- ,²⁹ leading to the formation of the *para* product (IV in Scheme 1). Note that I/II pair has the least $\Delta\omega$ value of 2.2324 eV and I/II–2 (II– AlCl_3) has the largest $\Delta\omega$ value of 8.1673 eV, consistent with our experimental findings that the I/II pair gives the lowest *p/m* regioselectivity of 2.6 and I/II–2 pair has the highest *p/m* regioselectivity ($p/m = 10.6$).⁵²

On the other hand, we notice that the f_k^+ value at the C3 atom in II is always higher than that in all II–LAs, implying that the C3 site of II is more electrophilic than that of all II–LAs. This result does not agree with the experimental result that an LA accelerates the reaction.⁵² But the local electrophilicity index ω_k value at the C3 atom on II is lower than that on II–LAs except II–3 (acrolein– FeCl_3) and II–5 (acrolein– CuCl_2). Because ω_k contains a global contribution of ω as a multiplicative factor of the local electrophilic index f_k^+ ,²⁹ it should be more appropriate and reliable than f_k^+ in analyzing the site activity and selectivity for electrophile–nucleophile reactions. It is interesting to notice that the difference of ω_k value ($\Delta\omega_k$ shown in Table 1) at C3 and C4 site on all II–LAs is larger

TABLE 1: Calculated DFT Reactivity Indices and the Frontier Molecular Orbital Energies for All Reactants at the B3LYP/6-311+g* Level (au)

	global properties					local properties				
	HOMO	LUMO	μ	η	ω	site	f_k^+	f_k^-	ω_k	$\Delta\omega_k^a$
I	-0.239	-0.037	-0.138	0.101	0.094	1	0.279	0.294	0.026	0.002
II	-0.273	-0.088	-0.180	0.092	0.176	2	0.263	0.250	0.025	
						3	0.346	0.176	0.061	0.047
						4	0.080	-0.006	0.014	
II-1	-0.279	-0.160	-0.219	0.060	0.403	3	0.307	0.066	0.124	0.122
						4	0.003	-0.012	0.001	
II-2	-0.296	-0.163	-0.229	0.067	0.394	3	0.315	0.053	0.124	0.123
						4	0.004	-0.009	0.002	
II-3	-0.296	-0.153	-0.224	0.071	0.353	3	0.153	0.068	0.054	0.060
						4	-0.018	0.002	-0.007	
II-4	-0.283	-0.147	-0.215	0.068	0.339	3	0.259	0.084	0.088	0.086
						4	0.004	-0.009	0.002	
II-5	-0.283	-0.150	-0.217	0.066	0.354	3	0.130	0.069	0.046	0.056
						4	-0.028	-0.012	-0.010	
II-6	-0.240	-0.142	-0.191	0.049	0.374	3	0.298	0.090	0.111	0.103
						4	0.023	-0.020	0.009	
II-7	-0.287	-0.145	-0.216	0.071	0.329	3	0.316	0.066	0.104	0.098
						4	0.020	-0.010	0.007	

^a $\Delta\omega_k = \omega_k(3) - \omega_k(4)$.

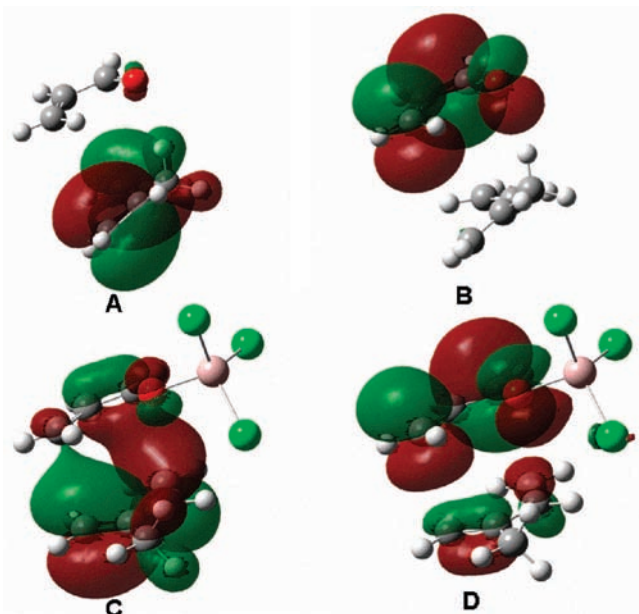


Figure 1. Comparison of the frontier orbitals for I/II (A, HOMO of I/II; B, LUMO of I/II) and I/II-AlCl₃ (C, HOMO of I/II-AlCl₃; D, LUMO of I/II-AlCl₃).

than that on II, exhibiting that these LA-catalyzed DA reactions have a large polar feature. In addition, similar to the $\Delta\omega$ value discussed above, the least $\Delta\omega_k$ value is also from II and the largest $\Delta\omega_k$ value from II-2, in consensus with the experimental results of their lowest *p/m* regioproduct ratio (*p/m* = 2.6) and highest *p/m* regioproduct ratio (*p/m* = 10.6), respectively.

To further investigate the effects of LAs on I/II DA reaction, the activation barrier ΔE_a as defined in eq 12 is analyzed. Because the activation barrier height is a good measurement of the catalytic activity, which evaluates how much acceleration is caused by a catalyst, the estimated ΔE_a can be regarded as an indication of catalytic activity. Figure 2 displays the linear relationship between ΔE_a and the ω value of dienophiles. Compared with II, the ΔE_a values of all II-LAs are always smaller, verifying the accelerating effect of the LAs for the reaction. The observed trend of catalytic strength of different LA catalysts is as follows: AlCl₃ > BCl₃ > FeCl₃ > CuCl₂ >

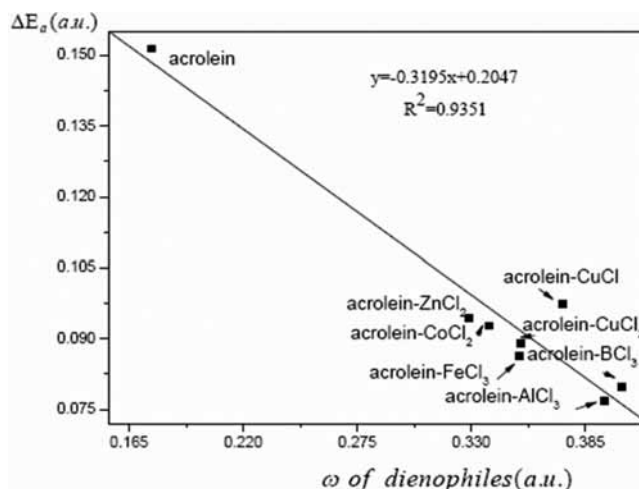


Figure 2. Linear relationship between the estimated activation barrier (ΔE_a) and electrophilicity index ω for acrolein and acrolein-LAs.

CoCl₂ > ZnCl₂ > CuCl, which is in agreement with the experimentally observed order reported in our previous study.⁵² The reason that acrolein-CuCl (II-6) looks to be an outlier in Figure 2 is because of its higher HOMO and LUMO energies compared with other II-LAs (see Table 1).

Quantitative relationships between structure and reactivity for II in the absence and presence of LAs are shown in Figure 3. It shows that the C=C bond order of II will become weakened and the C=C distance lengthened when the LA complex is formed. As Figure 2 has revealed, the electrophilicity index ω of different II-LAs is related to the catalytic activity. The decreased C=C bond order and increased C=C distance are strongly correlated to the catalytic activity order of II-LAs, indicating that upon complexation with LA, C=C is more prone to cleavage to form a new C-C bond with I.

Scheme 2 shows the geometric structure of complexation between II and LA. A few selected bond distances and angles from the optimized structures are tabulated in Table 2. A cyclic coplanar structure of II-LA with small Φ (-0.156 – -0.155°) is observed (see Scheme 2 and Table 2), consistent with earlier observations elsewhere.⁵³ As shown in Scheme 2, one of chlorine atoms of LA, together with the LA center, carbonyl

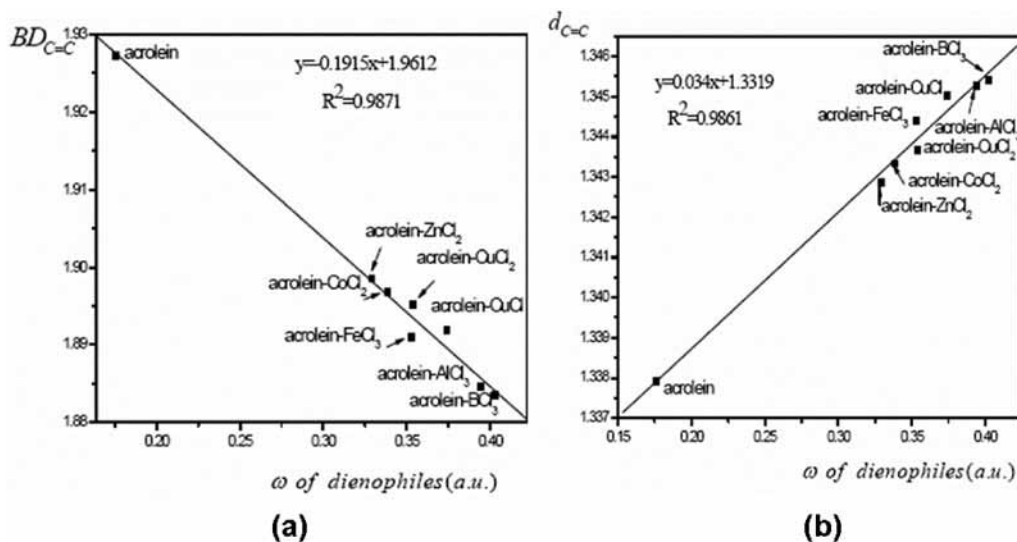
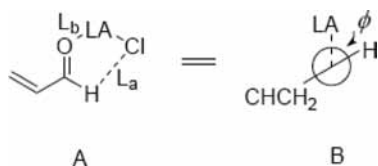


Figure 3. A linear correlation for (a) bond order of C3=C4 and ω of II and II-LAs; (b) distance of C3=C4 and ω of II and II-LAs.

SCHEME 2: Structure Observed from Complexation of Acrolein with LA



group, and aldehyde-H, form a planar five-membered ring. The hydrogen bonding formation between aldehyde-H and Cl (Scheme 2, A) is possible, which has also been confirmed by the stabilization interaction energies $E(2)$ analysis between aldehyde-H and Cl shown in Table 3. Also, notice in Table 2 that negative charges on carbonyl oxygen atom (Z_O) of II-LAs are similar except for the II- BCl_3 complex (II-1), which has the highest Z_O value. Besides, the smallest L_a , L_b , and Z_M values of II-1 are observed among all these II-LAs. The large bond order of 0.6567 between boron and carbonyl oxygen atoms from the NBO analysis is an indication of a strong interaction between II and BCl_3 .

The binding between II and LA (2-7) is believed to be electrostatically dominated because all of them have a large positive charge (Z_M) on the LA site. However, the Cu^+ cation ($Z_M(\text{Cu}^+) = 0.724$) is less positive than the rest because the CuCl catalyst has only one electron-withdrawing chlorine atom. The binding angle of $\text{Cl}-\text{Cu}-\text{O}$ (see Scheme 2A) is almost linear, 177.5° , and the L_a value of II- CuCl (II-6) is the largest ($L_a = 4.8241 \text{ \AA}$), making the hydrogen bonding interaction between aldehyde-H and Cl negligible. We will also confirm from the stabilization interaction energy $E(2)$ analysis of II- CuCl in Table 3 that no noticeable interaction between aldehyde-H and Cl has been found.

Table 3 displays the stabilization interaction energy for II-LAs from the NBO analysis. For II- BCl_3 (II-1), the strong donor-acceptor interaction occurs between $\text{C}=\text{O}$ and $\text{B}-\text{Cl}$ ($\text{BD C}=\text{O} \rightarrow \text{BD}^* \text{M}-\text{Cl}$, $\text{LP O} \rightarrow \text{BD}^* \text{M}-\text{Cl}$ and $\text{BD M}-\text{Cl} \rightarrow \text{BD}^* \text{C}=\text{O}$); however, there exists no interaction between boron and carbonyl oxygen atoms ($\text{BD C}=\text{O} \rightarrow \text{LP}^* \text{M}$, $\text{LP M} \rightarrow \text{BD}^* \text{C}=\text{O}$ and $\text{LP O} \rightarrow \text{LP}^* \text{M}$). Considering the strong bond order between boron and carbonyl oxygen atoms ($\text{BD}_{\text{B}-\text{O}} = 0.6567$), it strongly suggests that II and BCl_3 are covalently linked. For II-2 to II-5 complexes, there is a strong donor-acceptor interaction between the LP O orbital and the

$\text{LP}^* \text{M}$ orbital. For II-6 and II-7 complexes, the interaction between the donor LP O orbital and acceptor's $\text{BD}^* \text{M}-\text{Cl}$ is dominant, and the interaction between the donor carbonyl oxygen atom and acceptor LA center ($\text{BD C}=\text{O} \rightarrow \text{LP}^* \text{M}$ and $\text{LP O} \rightarrow \text{LP}^* \text{M}$) is negligible because the d-shell of both CuCl and ZnCl_2 is full, unable to accept extra electrons.

As shown above, the acrolein's carbonyl group in coordination with the LA catalyst activates the DA reaction and provides the catalytic power in cutting back the reaction barrier. Figure 4 exhibits the linear relationship between activation capability with electrophilicity index ω of LAs. Here, ΔE is the energy difference between LUMO_{LA} and $\text{HOMO}_{\text{acrolein}}$ from eq 13. It is seen that the larger the ω value of LA, the lower the ΔE value, and thus the more reactive the LA.

The DA reaction between I and II yields two main regioisomers, III and IV, with the latter as the major product from the experiments. Recently, Noorizadeh and Maihimi³⁶ showed that the major product of a DA reaction always has a smaller electrophilicity index than the minor product and claimed that electrophilicity index used as a global reactivity descriptor is better than hardness and polarizability to predict the regioselectivity, at least for this kind of reactions. We extend in this work their results to DA reactions with accelerating LA catalysts present. Shown in Table 4 are global hardness (η), polarizabilities (α), and electrophilicity indexes (ω) using eqs 3-6 to evaluate the stability for the two regioisomer products. According to MHP, MPP and MEP, a more reactive species (reactant or product) possesses a smaller η , larger α and larger ω , and conversely a more stable species has a larger η , smaller α and smaller ω . It is expected that the major regioproduct (*para*-substituted isomer, IV) should have a larger η and smaller α and ω . From Table 4, it is found that MHP correctly predicts the major regioisomer of LA-catalyzed DA reactions except for IV-6. MEP works for IV-2, IV-3 and IV-4, but MPP is invalid for all cases. These results suggest that using global descriptors hardness is better behaved in predicting the stability order of regioisomers for the LA catalyzed DA reaction systems.

When the difference measurement of MHP, MPP, and MEP defined in eq 11 is used, however, different results can be obtained. Table 5 shows the difference of hardness ($\Delta\eta$), polarizability ($\Delta\alpha$) and electrophilicity index ($\Delta\omega$) defined in eq 11 for the DA reactions. In this case, MHP becomes invalid because all the $\Delta\eta$ values are negative. Both $\Delta\alpha$ and $\Delta\omega$ are

TABLE 2: Some Selected Geometry Parameters for Acrolein–LA Complexes

	II-1	II-2	II-3	II-4	II-5	II-6	II-7
Φ (deg) ^a	0.0076	0.0038	−0.0028	0.1549	−0.1559	0.1380	0.0135
Z_M ^b	0.397	1.385	1.299	1.219	1.187	0.724	1.449
Z_O ^c	−0.548	−0.652	−0.633	−0.648	−0.634	−0.652	−0.678
L_a (Å) ^d	2.5194	2.7516	2.80852	2.7391	2.6683	4.82414	2.7461
L_b (Å) ^e	1.5969	1.9245	2.0294	1.9921	1.9120	1.7734	2.0424

^a Dihedral angle of LA–O=C–H shown in Scheme 2B. ^b NBO charge of LA center. ^c NBO charge of carbonyl oxygen atom. ^d Distance of carbonyl oxygen atom and LA center shown in Scheme 2A. ^e Distance of aldehyde–H and the coplanar chlorine atom of LA shown in Scheme 2A.

TABLE 3: Selected Stabilization Interaction Energies $E(2)$ for the Acrolein–LA Complexes (kcal/mol)

donor NBO → acceptor NBO	II-1	II-2	II-3	II-4	II-5	II-6	II-7
BD C=O → LP* M			14.03	0.67	2.49	2.28	
BD C=O → BD* M–Cl	4.22	2.66	1.91			4.1	0.93
LP O → LP* M			102.84	16.03	46.52	52.5	
LP O → BD* M–Cl	4.85	15.98		7.24	0.77	59.67	19.8
BD M–Cl → BD* C=O	2.98	0.26		0.27	0.06	0.07	0.19
LP M → BD* C=O				0.35	1.89	1.66	6.67
BD M–Cl → BD* C–H			0.08			0.04	0.08
LP Cl → BD* C–H	1.4	0.94	0.4	1.21	1.28		1.27

TABLE 4: Calculated Hardness Values (η), Polarizabilities (α) and Global Electrophilicity Indices (ω) of the Two Products Involved in DA Reactions at the B3LYP/6-311+g* Level (au)^a

	non-LA	1	2	3	4	5	6	7
η								
III–LA	0.102	0.076	0.075	0.079	0.081	0.080	0.067	0.082
IV–LA	0.104	0.077	0.080	0.083	0.082	0.081	0.066	0.083
α								
III–LA	94.1	150.5	153.9	175.1	151.4	159.7	139.1	142.6
IV–LA	95.3	152.3	154.9	177.1	178.9	162.1	141.2	143.9
ω								
III–LA	0.098	0.250	0.258	0.227	0.214	0.221	0.216	0.207
IV–LA	0.099	0.251	0.241	0.213	0.212	0.222	0.218	0.208

^a The maximum hardness, minimum polarizability and electrophilicity values are in bold fonts for each product.

TABLE 5: Differences of Hardness ($\Delta\eta$), Polarizability ($\Delta\alpha$) and Electrophilicity ($\Delta\omega$) between Reactants and Products (au)^a

	non-LA	1	2	3	4	5	6	7
$\Delta\eta$								
A ^b	−0.091	−0.085	−0.093	−0.093	−0.088	−0.088	−0.084	−0.090
B ^c	−0.090	−0.084	−0.089	−0.089	−0.088	−0.087	−0.084	−0.089
$\Delta\alpha$								
A ^b	−7.7	−8.8	−7.5	−7.8	−7.7	−5.6	−15.7	−7.0
B ^c	−6.5	−7.0	−6.5	−5.8	19.9	−3.2	−13.6	−5.7
$\Delta\omega$								
A ^b	−0.172	−0.247	−0.231	−0.220	−0.219	−0.227	−0.252	−0.216
B ^c	−0.171	−0.246	−0.247	−0.234	−0.221	−0.226	−0.251	−0.215

^a The minimum polarizability and electrophilicity values are in bold fonts for each reaction. ^b A is the reaction I + II–LA → III–LA. ^c B is the reaction I + II–LA → IV–LA.

less than zero, indicating that MPP and MEP can correctly predict the direction of the DA reaction, suggesting that the product possesses a smaller polarizability and electrophilicity.

But can MPP and MEP predict the preferred regioisomer product, *para*-substituted isomer IV? MPP cannot and MEP can do partially. For DA reactions with the same reactants but different products, the $\Delta\omega$ value toward to the preferred reaction pathway is anticipated to be smaller than the unfavorable pathway. The B reaction in Table 5 produces the major regioproduct IV, which, if MEP is applicable, should have a smaller $\Delta\omega$ value than the A reaction pathway. We observed this trend for three systems, IV–2, IV–3 and IV–4 (see Table 5). We can see that the $\Delta\omega$ value for reaction I + II–2 → IV–2 is smaller than that of reactions I + II–3 → IV–3 and I + II–4 → IV–4, meaning that the LA catalysts used in this DA reaction have a catalytic activity order of $\text{AlCl}_3 > \text{FeCl}_3 >$

CoCl_2 , which is in agreement with the LA catalytic activity order discussed above (see Figure 1). However, except for these three reactions, others seemingly do not obey what MEP predicts. The reason behind is likely that the difference in $\Delta\omega$ values of the two reaction pathways, A and B, are insignificant; the biggest difference is found to be just 0.0012 au (0.75 kcal/mol) for I + II–6 → III–6 and I + II–6 → IV–6.

Although in most cases MHP successfully predicts that DA reactions can favorably proceed, it is unable to predict the preferred reaction product in all of the considered reactions. MEP correctly predicts reaction trend, but it seems not to be so reliable in predicting the major regioisomer product and preferred reaction pathway for LA-catalyzed DA reactions. A number of reasons may have been contributed such as the gas-phase-like model, single-molecule approximation for the LA, etc. It may also have to do with the fact that the validity of

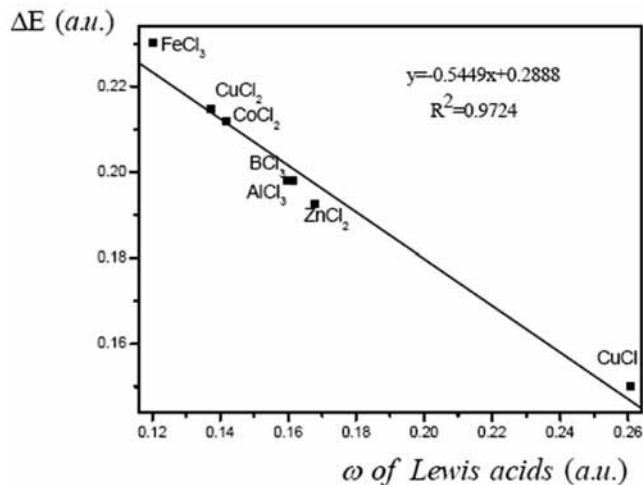


Figure 4. Linear relationship between the activation barrier of LAs (ΔE) and electrophilicity index ω of LAs.

MHP and others require that the external potential and chemical potential should be held constant during the evaluation process, which is often untrue for chemical reactions such as those considered here. Finally, we mention in passing that similar results (not shown here) have also been obtained with I and A approximated by the finite energy difference instead of HOMO/LUMO energies.

5. Conclusions

The impact of LA catalysts applied to a normal electron demand Diels–Alder reaction system (isoprene/acrolein) has been investigated using DFT and conceptual DFT (also called Chemical DFT⁵⁴) approaches. We found that the complexation of dienophile (acrolein) with LA significantly decreases the LUMO energy of acrolein and increases the electrophilicity of acrolein. We also observed noticeable difference in the shape and localization of HOMO and LUMO distribution. Structure analysis of the acrolein–LA complex finds a planar five-membered ring formed by the chlorine atom, LA center, carbonyl group and aldehyde–H. NBO analysis results indicate two different kinds of interactions between acrolein and LAs, one in covalent bonding nature and the other dominated by electrostatic interactions. Catalytic activities of different LAs have been estimated via frontier molecular orbitals and found to be consistent with experiments. A few linear relationships have been established between structure and reactivity properties, such as bond order, bond length, catalytic activity, and reactivity indices. Finally, we discussed the validity and applicability of the maximum hardness principle (MHP), minimum polarizability (MPP) and minimum electrophilicity principles (MEP) for the systems. We found that MHP can usually predict the major regioisomer products of a DA reaction, but it fails to predict the reaction direction. MPP is able to forecast the reaction direction but fails in predicting the major regioselective isomer. MEP can do both but cannot do so always.

Acknowledgment. We are grateful to the Virtual Laboratory for Computational Chemistry, Computer Network Information Center, Chinese Academy of Sciences, for allowing us to access its computing facilities for the present study.

References and Notes

(1) Carruthers, W. *Cycloaddition Reactions in Organic Synthesis*; Pergamon Press: Oxford U.K., 1990.

- (2) Fringuelli, F.; Taticchi, A. *The Diels–Alder Reaction: Selected Practical Methods*; John Wiley & Sons, Ltd.: New York, 2002.
- (3) Kumar, A. *Chem. Rev.* **2001**, *101*, 1.
- (4) Takao, K.; Munakata, R.; Tadano, K. *Chem. Rev.* **2005**, *105*, 4779.
- (5) Martin, J. G.; Hill, R. K. *Chem. Rev.* **1961**, *61*, 537.
- (6) Houk, K. N. *J. Am. Chem. Soc.* **1973**, *95*, 4092.
- (7) Houk, K. N. *Acc. Chem. Rev.* **1975**, *8*, 361.
- (8) Fleming, I. *Frontier Orbitals and Organic Chemical Reaction*; Wiley: Chichester, U.K., 1976.
- (9) Kahn, S. D.; Pau, C. F.; Overman, L. E.; Hehre, W. J. *J. Am. Chem. Soc.* **1986**, *108*, 7381.
- (10) Alston, P. V.; Ottenbrite, R. M.; Shillady, D. D. *J. Org. Chem.* **1973**, *38*, 4075.
- (11) Yates, P.; Eaton, P. *J. Am. Chem. Soc.* **1960**, *82*, 4436.
- (12) Kagan, H. B.; Riant, O. *Chem. Rev.* **1992**, *92*, 1007.
- (13) Pindur, U.; Lutz, G.; Otto, C. *Chem. Rev.* **1993**, *93*, 741.
- (14) Houk, K. N.; Strozier, R. W. *J. Am. Chem. Soc.* **1973**, *95*, 4094.
- (15) Alston, P. V.; Ottenbrite, R. M. *J. Org. Chem.* **1975**, *40*, 1111.
- (16) Alves, C. N.; da Silva, A. B. F.; Martf, S.; Moliner, V.; Oliva, M.; Andrés, J.; Domingo, L. R. *Tetrahedron* **2002**, *58*, 2695.
- (17) Birney, D. M.; Houk, K. N. *J. Am. Chem. Soc.* **1990**, *112*, 4127.
- (18) Yamabe, S.; Dai, T.; Minato, T. *J. Am. Chem. Soc.* **1995**, *117*, 10994.
- (19) Yamabe, S.; Minato, T. *J. Org. Chem.* **2000**, *65*, 1830.
- (20) García, J. I.; Martínez-Merino, V.; Mayoral, J. A.; Salvatella, L. *J. Am. Chem. Soc.* **1998**, *120*, 2415.
- (21) Berski, S.; Andrés, J.; Silvi, B.; Domingo, L. R. *J. Phys. Chem. A* **2006**, *110*, 13939.
- (22) Ess, D. H.; Jones, G. O.; Houk, K. N. *Adv. Synth. Catal.* **2006**, *348*, 2337.
- (23) Parr, R. G.; Yang, W. *Density Functional Theory of Atoms and Molecules*; Oxford University Press: Oxford, U.K., 1989.
- (24) Geerlings, P.; De Proft, F.; Langenaeker, W. *Chem. Rev.* **2003**, *103*, 1793.
- (25) Parr, R. G.; Szentpály, L. V.; Liu, S. B. *J. Am. Chem. Soc.* **1999**, *121*, 1922.
- (26) Chattaraj, P. K.; Sarkar, U.; Roy, D. R. *Chem. Rev.* **2006**, *106*, 2065.
- (27) Chattaraj, P. K.; Roy, D. R. *Chem. Rev.* **2007**, *107*, PR46.
- (28) Domingo, L. R.; Aurell, M. J.; Pérez, P.; Contreras, R. *Tetrahedron* **2002**, *58*, 4417.
- (29) Domingo, L. R.; Aurell, M. J.; Prez, P.; Contreras, R. *J. Phys. Chem. A* **2002**, *106*, 6871.
- (30) Damoun, S.; Van de Woude, G.; Mndez, F.; Geerlings, P. *J. Phys. Chem. A* **1997**, *101*, 886.
- (31) Chattaraj, P. K.; Liu, G. H.; Parr, R. G. *Chem. Phys. Lett.* **1995**, *237*, 171.
- (32) Chattaraj, P. K.; Sengupta, S. *J. Phys. Chem.* **1996**, *100*, 16126.
- (33) Liu, S. B.; Parr, R. G. *J. Chem. Phys.* **1997**, *106*, 5578.
- (34) Ayers, P. W.; Parr, R. G. *J. Am. Chem. Soc.* **2000**, *122*, 2010.
- (35) Chattaraj, P. K.; Maiti, B. *J. Am. Chem. Soc.* **2003**, *125*, 2705.
- (36) Chamorro, E.; Chattaraj, P. K.; Fuentealba, P. *J. Phys. Chem. A* **2003**, *107*, 7068.
- (37) Noorizadeh, S.; Maihami, H. *J. Mol. Struct. (THEOCHEM)* **2006**, *763*, 133.
- (38) Noorizadeh, S. *Chin. J. Chem.* **2007**, *25*, 1439.
- (39) Noorizadeh, S. *J. Phys. Org. Chem.* **2007**, *20*, 514.
- (40) Elango, M.; Parthasarathi, R.; Subramanian, V.; Chattaraj, P. K. *J. Mol. Struct. (THEOCHEM)* **2007**, *820*, 1.
- (41) Janak, J. F. *Phys. Rev. B* **1978**, *18*, 7165.
- (42) Parr, R. G.; Yang, W. *J. Am. Chem. Soc.* **1984**, *106*, 4049.
- (43) Yang, W.; Mortier, W. J. *J. Am. Chem. Soc.* **1986**, *108*, 5708.
- (44) Li, X. Y.; Nie, J. *J. Phys. Chem. A* **2003**, *107*, 6007.
- (45) Rong, C. Y.; Lian, S. X.; Yin, D. L.; Zhong, A. G.; Zhang, R. Q.; Liu, S. B. *Chem. Phys. Lett.* **2007**, *434*, 149.
- (46) Guell, M.; Luis, J. M.; Sola, M.; Swart, M. *J. Phys. Chem. A* **2008**, *112*, 6384.
- (47) Rong, C. Y.; Lian, S. X.; Yin, D. L.; Shen, B.; Zhong, A. G.; Bartolotti, L.; Liu, S. B. *J. Chem. Phys.* **2006**, *125*, 174102.
- (48) Huang, Y.; Zhong, A. G.; Rong, C.; Xiao, X. M.; Liu, S. B. *J. Phys. Chem. A* **2008**, *112*, 305.
- (49) Liu, S. B.; Langenaeker, W. *Theor. Chem. Acc.* **2003**, *110*, 338.
- (50) Zhong, A. G.; Liu, S. B. *J. Theor. Comput. Chem.* **2005**, *4*, 833.
- (51) Frisch, M. J.; Trucks, G. W.; Schlegel, H. B.; Scuseria, G. E.; Robb, M. A.; Cheeseman, J. R.; Montgomery, J. A., Jr.; Vreven, T.; Kudin, K. N.; Burant, J. C.; Millam, J. M.; Iyengar, S. S.; Tomasi, J.; Barone, V.; Mennucci, B.; Cossi, M.; Scalmani, G.; Rega, N.; Petersson, G. A.; Nakatsuji, H.; Hada, M.; Ehara, M.; Toyota, K.; Fukuda, R.; Hasegawa, J.; Ishida, M.; Nakajima, T.; Honda, Y.; Kitao, O.; Nakai, H.; Klene, M.; Li, X.; Knox, J. E.; Hratchian, H. P.; Cross, J. B.; Adamo, C.; Jaramillo, J.; Gomperts, R.; Stratmann, R. E.; Yazyev, O.; Austin, A. J.; Cammi, R.; Pomelli, C.; Ochterski, J. W.; Ayala, P. Y.; Morokuma, K.; Voth, G. A.; Salvador, P.; Dannenberg, J. J.; Zakrzewski, V. G.; Dapprich, S.; Daniels,

A. D.; Strain, M. C.; Farkas, O.; Malick, D. K.; Rabuck, A. D.; Raghavachari, K.; Foresman, J. B.; Ortiz, J. V.; Cui, Q.; Baboul, A. G.; Clifford, S.; Cioslowski, J.; Stefanov, B. B.; Liu, G.; Liashenko, A.; Piskorz, P.; Komaromi, I.; Martin, R. L.; Fox, D. J.; Keith, T.; Al-Laham, M. A.; Peng, C. Y.; Nanayakkara, A.; Challacombe, M.; Gill, P. M. W.; Johnson, B.; Chen, W.; Wong, M. W.; Gonzalez, C.; Pople, J. A. Gaussian 03, revision B.04; Gaussian, Inc. Pittsburgh, PA, 2003.

(52) Yin, D. H.; Yin, D. L.; Fu, Z. H.; Li, Q. H. *J. Mol. Catal. A: Chem.* **1999**, 148, 87.

(53) Woodward, S. *Tetrahedron* **2002**, 58, 1017.

(54) Ayers, P. W.; Parr, R. G. *J. Chem. Phys.* **2008**, 128, 184108.

JP805410C